Revista Brasileira de Climatologia
Brazilian Journal of Climatology

OPEN ACCESS

BIBLIOTECA Coordenadoria de Bibliotecas Portal de Periódicos
ISSN 2237-8642

PRECIPITATION DYNAMICS IN FORESTS AND DEFORESTATION AREAS DURING THE DRY SEASON IN THE CENTRAL-EASTERN AMAZON: A CASE STUDY IN THE XINGU BASIN

Dinâmica da precipitação em florestas e áreas de desmatamento durante a estação seca na Amazônia Centro-Leste: um estudo de caso na bacia do Xingu

Dinámica de la precipitación en bosques y áreas desforestadas durante la estación seca en la Amazonía Centro-Oriental: un estudio de caso en la cuenca del Xingu

Rodrigo Martins Moreira
Federal University of Rondônia (UNIR)
rodrigo.moreira@unir.br

Bruno César dos Santos
Federal University de São Carlos
bcsantos@ufscar.br

Abstract: The precipitation regimen in the Xingu watershed is an important aspect of the Amazon regional climate. In this paper, we analyze trends and extreme precipitation events in forested and deforested areas for the Xingu watershed, eastern Amazon. The estimated data was validated using rain gauges and statistical methods were applied to evaluate trends in precipitation patterns and spatialize the Sen's slope to provide insights for water resources management in the region for the dry season. The analysis employs Point-Biserial correlation tests to assess the association between binary forest cover (1 for forest, 0 for deforested) and various precipitation indexes. All stations with significant Mann-Kendall test showed decreasing precipitation, and the largest precipitation reduction trend found was -0.43 mm per month for station 151003. The results of the RPB correlation suggest that forest cover is more strongly associated with the persistence and intensity of wet periods than with isolated extreme precipitation events, shedding light on the interaction between precipitation patterns and forest dynamics.

Keywords: Climate change; Deforestation; Cloud Computing; Sen's Slope; Trends.

Resumo: O regime de precipitação na bacia do Xingu é um aspecto importante do clima regional da Amazônia. Neste artigo, analisamos tendências e eventos extremos de precipitação em áreas florestadas e de desmatamento da bacia do Xingu, na Amazônia oriental. Os dados estimados foram validados utilizando pluviômetros, e métodos estatísticos foram aplicados para avaliar as tendências nos padrões de precipitação e espacializar a inclinação de Sen para fornecer insights para a gestão dos recursos hídricos na região durante a estação seca. A análise emprega testes de correlação Ponto-Bisserial para avaliar a associação entre a cobertura florestal binária (1 para floresta, 0 para não floresta) e diversos índices de precipitação. Todas as estações com teste Mann-Kendall significativo apresentaram diminuição da precipitação, e a maior tendência de redução de precipitação encontrada foi de -0,43 mm por mês para a estação 151003. Os resultados da correlação RPB sugerem que a cobertura florestal está mais fortemente associada à persistência e à intensidade de períodos úmidos do que a eventos extremos isolados de precipitação, lançando luz sobre a interação entre os padrões de precipitação e a dinâmica florestal.

Palavras-chave: Mudança climática; Desmatamento; Computação em nuvem; Inclinação de Sen; Tendências.

Resumen: El régimen de precipitación en la cuenca del Xingu es un aspecto importante del clima regional de la Amazonía. En este artículo, analizamos tendencias y eventos extremos de precipitación en áreas boscosas y deforestadas de la cuenca del Xingu, en la Amazonía oriental. Los datos estimados fueron validados utilizando pluviómetros, y se aplicaron métodos estadísticos para evaluar las tendencias en los patrones de precipitación y espacializar la pendiente de Sen para ofrecer información útil para la gestión de los recursos hídricos en la región durante la estación seca. El análisis emplea pruebas de correlación punto-biserial para evaluar la asociación entre la cobertura forestal binaria (1 para bosque, 0 para no bosque) y diversos índices de precipitación. Todas las estaciones con prueba de Mann-Kendall significativa presentaron disminución de la precipitación, y la mayor tendencia de reducción encontrada fue de -0,43 mm por mes para la estación 151003. Los resultados de la correlación RPB sugieren que la cobertura forestal está más fuertemente asociada con la persistencia y la intensidad de los períodos húmedos que con eventos extremos aislados de precipitación, arrojando luz sobre la interacción entre los patrones de precipitación y la dinámica forestal.

Palabras clave: Cambio climático; Deforestación; Computación en la nube; Pendiente de Sen; Tendencias.

Submetido em: 27/08/2024
Aceito para publicação em: 04/06/2025
Publicado em: 03/07/2025

1. INTRODUCTION

Recognized as the largest remaining tropical forest on the planet, the Amazon also records the highest annual deforestation rates among tropical forests. In the eastern part of the Amazon, the Xingu River Basin covers around 500,000 km2 and has an average yearly discharge of approximately 8000 $m^3.s^{-1}$, ranking it as the Amazon's fifth largest tributary (Dias *et al*., 2015). Precipitation plays a critical role in sustaining the rainforest's hydrological cycle, which in turn supports the region's rich biodiversity. Climate change, however, has led to changes in precipitation patterns and extreme climatic events that may have significant implications for the Amazon rainforest's ecosystems and its inhabitants (Soares-Filho *et al*., 2012; Rizzo *et al*., 2020).

The Xingu Basin faces several environmental threats that can significantly impact the region's biodiversity and hydrological cycle. Deforestation, mining, and agriculture are some of the main drivers of environmental degradation in the basin (Souza, 2020). These activities can lead to soil erosion, loss of vegetation cover, and water pollution, among other impacts (Haghtalab *et al*., 2020). Changes in precipitation patterns and trends can exacerbate the environmental threats faced by the Xingu Basin. Climate change has led to changes in precipitation patterns in the Amazon region, with some areas experiencing more frequent extreme climatic events, such as severe droughts and floods (De Sales *et al*., 2020). This can further exacerbate the impact of deforestation, as the loss of vegetation cover can reduce the soil's water retention capacity, making the region more vulnerable to droughts and other climate extremes (Rizzo *et al*., 2020).

Changes in precipitation patterns can impact water resources, which are essential for the ecosystem and population of the Xingu River region (Lucas *et al*., 2021). Monitoring precipitation extremes is therefore of great importance in the Xingu watershed and the Amazon region. However, the existing rain gauge network in the Xingu watershed, a critical area for the region's biodiversity, is sparse and geographically limited. Remotely sensed precipitation products are thus necessary to supplement the limited rainfall data, and offer several advantages over rain gauge measurements, including broader spatial coverage, higher temporal resolution, and cost-effectiveness (Cavalcante *et al*., 2020). Various remote sensing products are available for estimating precipitation, including the Tropical Rainfall Measuring Mission (TRMM), Global Precipitation Measurement (GPM), and Climate Hazards group

InfraRed Precipitation with Station data (CHIRPS) (De Moraes Cordeiro; Blanco, 2021). Among these, CHIRPS has been widely used for precipitation monitoring and climate studies, due to its high accuracy, long-term data availability, and daily temporal resolution (De Sales *et al*., 2020).

In this scenario, statistical methods such as the Sen's Slope have been widely used to analyze magnitude of trends in precipitation patterns, not only in the Amazon region but also in other parts of the world. Spatialization of the Sen's Slope has also been recognized as a valuable tool for decision-making in water resources management, providing valuable information on precipitation trends across a particular area (Mu; Biggs; Shen, 2021). The utilization of the Sen's slope estimator in climate science studies highlights its importance in quantifying and assessing precipitation magnitude of change (De Moraes Cordeiro; Blanco, 2021). This statistical method enables researchers to identify both upward and downward trends, providing valuable information for climate studies, water resource management, and ecosystem monitoring (Cavalcante *et al*., 2020). By identifying and quantifying trends, these methods contribute to a better understanding of climate dynamics and assist in decision-making processes related to water resources and environmental management (Paca *et al*., 2020).

Alongside trend analysis, precipitation indices provide valuable information about different aspects of extreme precipitation events, including duration, intensity, frequency, and magnitude. Key precipitation indices commonly used in climate sciences are consecutive wet days (CWD), consecutive dry days (CDD), maximum 1-day precipitation (RX1), maximum 5-day precipitation (RX5), and the 99th percentile of daily precipitation (p99) (Cavalcante *et al*., 2020). Consecutive wet days (CWD) and consecutive dry days (CDD) are indices that quantify the duration of wet and dry periods, respectively (Lucas *et a*l., 2021). This work innovates by calculating these indexes using Google Earth Engine processing power, harvesting the potential of the free of cost and petabytes of data cloud computing platform.

In this paper, we present a spatial and temporal analysis of precipitation patterns in the Xingu watershed, using remotely sensed data from CHIRPS. We apply statistical methods to evaluate trends in precipitation patterns and spatialize the Sen's slope to provide insights for water resources management in the region. Our study highlights the importance of remote

sensing for precipitation monitoring in areas with limited rainfall data and provides valuable information for decision-making in water resources management in the Xingu watershed.

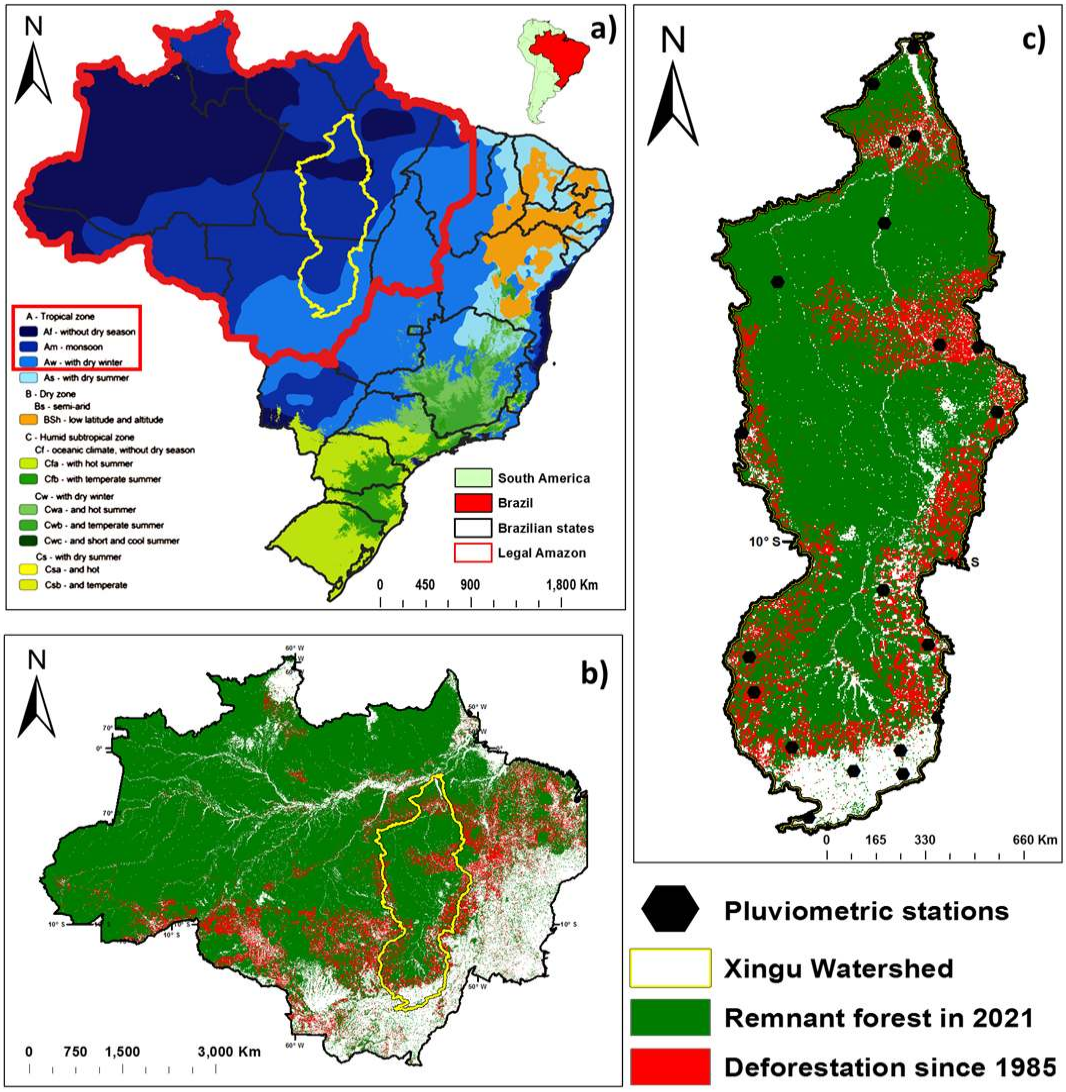
2. MATERIAL AND METHODS

2.1. Study area

The Xingu watershed is a significant river basin located in Brazil, covering a vast area in the Amazon rainforest. It is characterized by a diverse range of ecosystems, including forests, savannas, and wetlands.

The Xingu Watershed exhibits a tropical climate, as indicated by the Koppen-Geiger climate classification system, as shown in Figure 1. The majority of the Xingu Watershed falls under the Af climate type, which represents a hot and humid tropical climate with no dry season. This classification is consistent with the overall climate of the Amazon rainforest region, characterized by high temperatures and abundant rainfall throughout the year.

Figure 1 - Location of the study area (in yellow): a) Koppen climate classification; b) Deforestation in the Legal Amazon since 1985; c) Location of selected rain gauges within the Xingu watershed.



Source: MapBiomas (2021) e Alvares (2013).

2.2 CHIRPS precipitation data

To obtain the precipitation data, the CHIRPS (Climate Hazards Group InfraRed Precipitation with Station data) dataset was used (Funk *et al*., 2015). CHIRPS combines satellite-based precipitation estimates with ground-based rain gauge observations. This approach overcomes the limitations of each data source when used independently by capitalizing on their respective strengths. Satellite-based estimates fill in data gaps where rain gauges are scarce or nonexistent, while rain gauges provide ground truth data to enhance the accuracy of satellite-based estimates. As a result, CHIRPS produces high-quality, high-resolution precipitation data at a resolution of 0.05°. This dataset has diverse applications, including drought monitoring and flood forecasting. The methodology employed in CHIRPS is

described in detail in Funk et al. (2015), and its reliability has been extensively tested and validated in various regions worldwide.

To analyze historical precipitation data in the Xingu basin, rainfall indices and trend analysis tools were used. These methods were applied on a pixel-by-pixel scale. The CHIRPS data were processed at a daily scale for the dry season period, covering the months from May to October.

2.3. Calculation of precipitation indexes in GEE

CWD represents the maximum number of consecutive days with precipitation above a specified threshold (e.g., 0.1 mm). An algorithm was developed to iterate through the dataset and count the number of consecutive days with precipitation above the threshold. The maximum count of consecutive wet days was recorded as CWD. The function to calculate this index in GEE was by identifying the values above zero in every image on the image collection - ImageCollection.gt(0) - over the CHIRPS Daily image collection.

CDD refers to the maximum number of consecutive days with precipitation below a specified threshold (e.g., 0.1 mm). Similar to the CWD calculation, the algorithm counted the number of consecutive days with precipitation below the threshold, and the maximum count was recorded as CDD. The function to calculate this index in GEE was by identifying the values equal to zero in every image on the image collection - ImageCollection.eq(0) - over the CHIRPS Daily image collection.

RX1 represents the maximum amount of precipitation recorded within a single day during the analysis period. The algorithm identified the highest value from the daily precipitation data and assigned it as RX1. The function to calculate this index in GEE was ImageCollection.max() over the CHIRPS Daily image collection.

RX5 represents the maximum accumulated precipitation over any 5 consecutive days during the analysis period. A moving window of 5 days was applied to the dataset, and the total precipitation within each window was calculated. The maximum value obtained from the 5-day windows was assigned as RX5. The function to calculate this index in GEE was ImageCollection.max() over the CHIRPS Pentad image collection.

The p99 represents the precipitation value below which 99% of the daily precipitation data falls. The algorithm sorted the daily precipitation values in ascending order and identified

the value at the 99th percentile. This value was assigned as p99. The function to calculate this index in GEE by passing ee.Reducer.percentile(99) over the image collection time series.

2.4. Sen's Slope Analysis

Once significant trends have been identified, it is important to estimate the magnitude of this trend. For the test, the annual temporal scale was used. In the various methods applied for this purpose, the normality of the dataset is a prerequisite, being highly sensitive to outliers. To overcome this limiting factor, it is necessary to apply a more robust test adapted to non-parametric data, such as Sen's Slope (SS), aimed at identifying magnitudes in time series trends (Equation (1)).

$$SS = Median\left\{\left[\left(\frac{x_i - x_j}{i-j}\right)_{j=1}^{j=n-1}\right]_{i=j+1}^{i=n}\right\}$$

where xi and xj are pairs at given times i and j (j > i), respectively.

The Sen's Slope was calculated in a monthly precipitation sum time scale using ee.Reducer.sensSlope().

2.5. Point-biserial correlation

Point-biserial correlation, often denoted as RPB, is a statistical measure used to assess the strength and direction of the relationship between a binary variable (in this study, forest and deforested) and a continuous variable. It is a specialized form of correlation that quantifies the association between these two types of variables.

The point-biserial correlation coefficient falls within the range of -1 to 1, with negative values indicating a negative relationship, positive values indicating a positive relationship, and zero indicating no relationship.

The formula for calculating the point-biserial correlation is as follows (Equation (2)):

$$r_{pb} = \frac{M_0 - M_1}{s_y}\sqrt{\frac{n_0 \cdot n_1}{n^2}}$$

Where:

M_1 is the mean of the continuous variable for the group with a value of 1 (forest).

M_0 is the mean of the continuous variable for the group with a value of 0 (deforested).

s is the standard deviation of the continuous variable for the entire sample.

n_1 is the sample size of the group with a value of 1.

n_0 is the sample size of the group with a value of 0.

N is the total sample size.

The interpretation of the point-biserial correlation coefficient depends on its magnitude (Tate, 1954):

A positive point-biserial correlation ($r_{pb}>0$) indicates that as the binary variable increases (e.g., from 0 to 1), the continuous variable tends to increase as well.

A negative point-biserial correlation ($r_{pb}<0$) indicates that as the binary variable increases, the continuous variable tends to decrease.

A point-biserial correlation of 0 ($r_{pb}=0$) suggests no linear relationship between the binary and continuous variables.

3. RESULTS

3.1. Dry season analysis

The following Table 1 summarizes the dry season precipitation trend values between stations within the Xingu basin. Between seasons, about 63.6% show that there is no change in precipitation trends, and about 36.3% show a decreasing trend for the dry period in the Xingu basin. Thus, the rainfall pattern during the dry period is maintained in most stations. However, some are showing a pattern of reduction, which may prolong the dry period in these places within the Xingu watershed.

Table 1 - Trend of dry season precipitation by means of Mann-Kendall (MK) between selected stations.

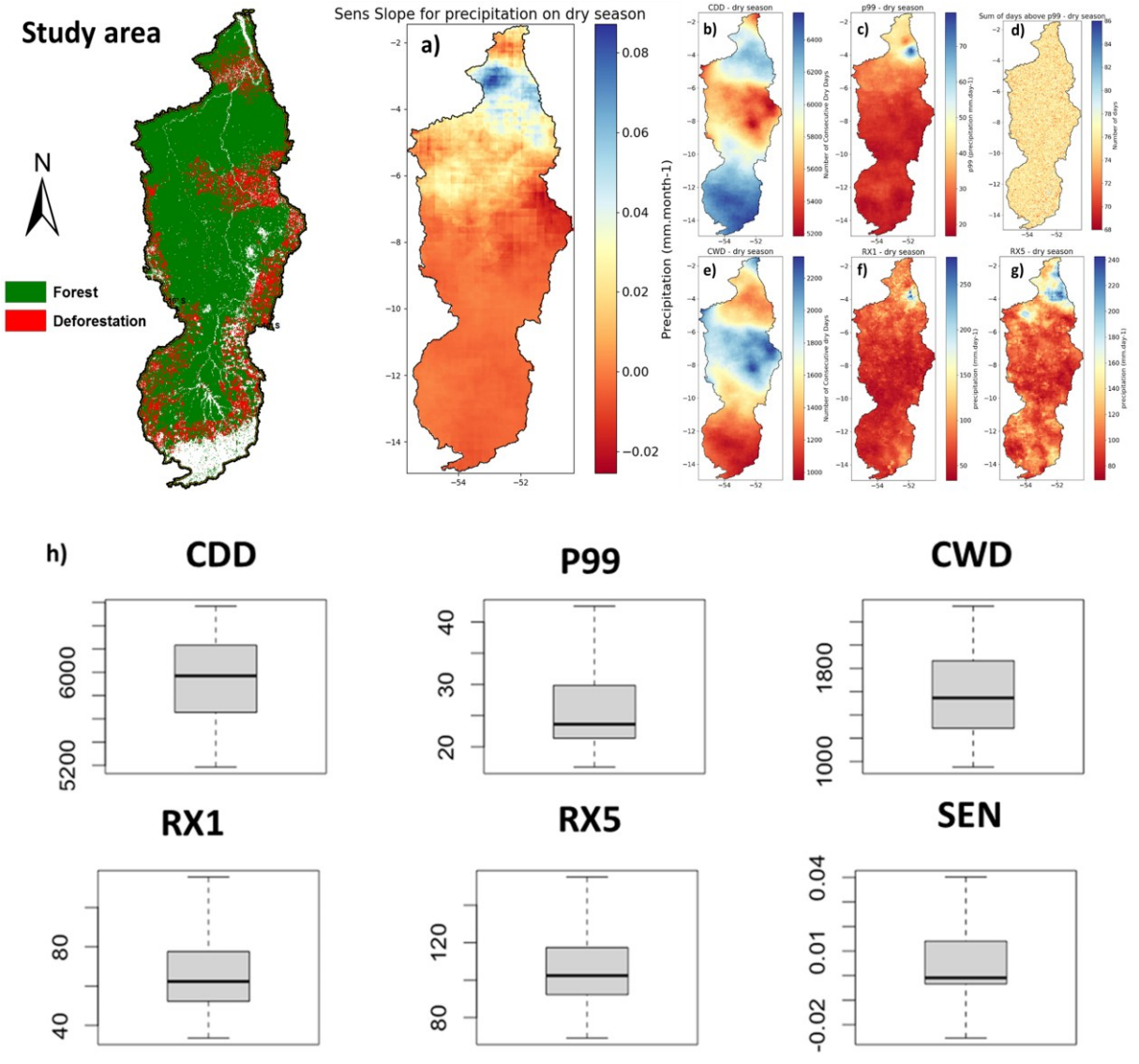
Rain Gauge Code	MK trend dry season	MK p-value dry season	MK slope dry season
151003	decreasing	0.000	-0.429
152001	no trend	0.296	0.096
252001	decreasing	0.012	-0.164
351002	no trend	0.807	0.012
352001	no trend	0.092	0.087
352005	no trend	0.633	-0.027
452000	no trend	0.935	-0.003
554000	decreasing	0.013	-0.125
651001	no trend	0.725	-0.015
651002	no trend	0.947	-0.001
750000	decreasing	0.002	-0.184
855000	no trend	0.259	0.007
1052000	no trend	0.685	0.000
1152000	no trend	0.838	0.000
1154001	no trend	0.062	0.000
1251001	no trend	0.193	0.000
1255002	no trend	0.202	0.000
1352000	decreasing	0.001	0.000
1352001	decreasing	0.007	0.000
1353001	decreasing	0.000	-0.044
1354000	no trend	0.623	0.000
1453000	decreasing	0.035	0.000

Source: Prepared by the authors (2023)

Figure 2 presents the daily precipitation trends during the dry season in the Xingu basin, based on different indices (CDD, CWD, RX1, RX5, P99) and the Sen Slope. In Figure 2a, a slight increase in precipitation is observed in the northern portion of the basin. In contrast,

the eastern region shows a slight tendency for a reduction in rainfall volumes. In general, most of the Xingu basin maintains a trend pattern considered usual for the dry season, with no significant changes.

Figure 2 – Map of the rainfall trend (dry season) of the applied rainfall indexes in the study area: a) Precipitation value (mm); b) Consecutive dry days; c) Precipitation value (mm) above 99%; d) Sum of days with precipitation value above 99%; e) Consecutive dry days; f) Maximum value (mm) of precipitation in one day; g) Maximum value (mm) of precipitation in five days; h) Boxplot dry season índices.



Source: Prepared by the authors (2023)

Between consecutive dry (Fig 2b) and wet (Fig 2e) days, an opposite pattern was observed in the Xingu basin. In the northern and southern regions of the basin, dry days (CDD) increased, while wet days (CWD) decreased. In the central portion, an opposite pattern was

observed, with a decrease in drought (CDD) for the frequency of wet days (CWD) in this region of the basin. The number of consecutive dry days is increasing in these areas (north and south) and, therefore, resulting in a lower frequency of wet days in this region of the basin. In the central portion of the basin, a different pattern was observed, with a reduction in CDD and an increase in CWD. This indicates that this part of the basin presents more wet days than dry days during the dry period, especially in the more central-eastern region, where trends point to a more significant increase in the basin.

Regarding the trends of the highest volume of rain in a single day (Fig 2f), there was a considerable reduction for almost the entire basin, with the exception of a small area to the north that showed an increase. As for the five-day cumulative rainfall trends (Fig 2g), the entire basin region recorded an overall reduction, but with a pattern of increase in five-day cumulative rainfall in the northeast portion of the basin.

Finally, extreme rainfall trends (volumes 99% above average) showed a general reduction in volume (Fig 2c) for almost the entire basin, mainly in the central-southern portion. However, the northern part showed an increase in the volume of extreme rainfall in an isolated area to the northeast of the basin. As for the number of days of extreme rain (Fig 2d), on average, the basin records about 76 days of rainfall with volumes above 99% in relation to the average during the wet period.

Figure 2h at the bottom of the image shows the variation in precipitation values (mm or days) in the dry period between rainfall indices and also the rainfall trend. Regarding the CDD and CWD indices, the results show an average number of days of approximately 5,900 for consecutive dry days and approximately 1,500 for consecutive wet days. The range of days showed a variation of consecutive dry days (5,200 to 6,500 days) greater than the variation of consecutive wet days (900 to 2,300 days). For the RX1 and RX5 indices, the results show an average volume of precipitation of approximately 60mm, accumulated in one day, and approximately 100mm, accumulated in five days. The amplitude in millimeters ranged from 30 to 110mm for RX1 day and from 70 to 170mm for RX5 days. The P99 index results show an average extreme rainfall volume of 24mm and an amplitude between 17 and 42mm. Finally, the precipitation trend in the dry period showed no change on average (0.00) and in amplitude there were moments of trends with a slight reduction (-0.03) and a slight increase (0.04) in rain.

3.2. Point-biserial for forest and deforested areas

The point-biserial correlation analysis reveals statistically significant relationships between several climate-related variables and the presence of forest cover (Table 2).

Table 2 - Values for Point-biserial analysis.

Variable	Correlation	p-value
CDD	-0.146	0.000
CWD	0.149	0.000
above_p99	-0.029	0.004
precipitation_p99	0.152	0.000
RX1	-0.018	0.071
RX5	-0.159	0.000

Source: Prepared by the authors (2023)

Among the most notable results, RX5 (the maximum 5-day precipitation) exhibited the strongest correlation with forest cover ($r = -0.159$, $p < 0.001$). This negative association suggests that areas with forest cover tend to experience lower short-term extreme precipitation events compared to non-forested areas. Similarly, CDD (consecutive dry days) was also negatively correlated with forest cover ($r = -0.146$, $p < 0.001$), indicating that forests are less likely to occur in regions prone to prolonged dry spells. These findings support the idea that forested areas may play a buffering role in hydrological extremes, potentially due to their influence on microclimatic conditions and soil moisture retention.

Conversely, CWD (consecutive wet days) and precipitation_p99 (the 99th percentile of daily precipitation) both showed positive correlations with forest cover ($r = 0.149$ and $r = 0.152$, respectively; $p < 0.001$). These results suggest that forested areas are more likely to coincide with regions experiencing sustained wet periods and greater intensity of extreme precipitation events. This aligns with ecological theories that associate forest persistence with consistent moisture availability and favorable hydrological regimes.

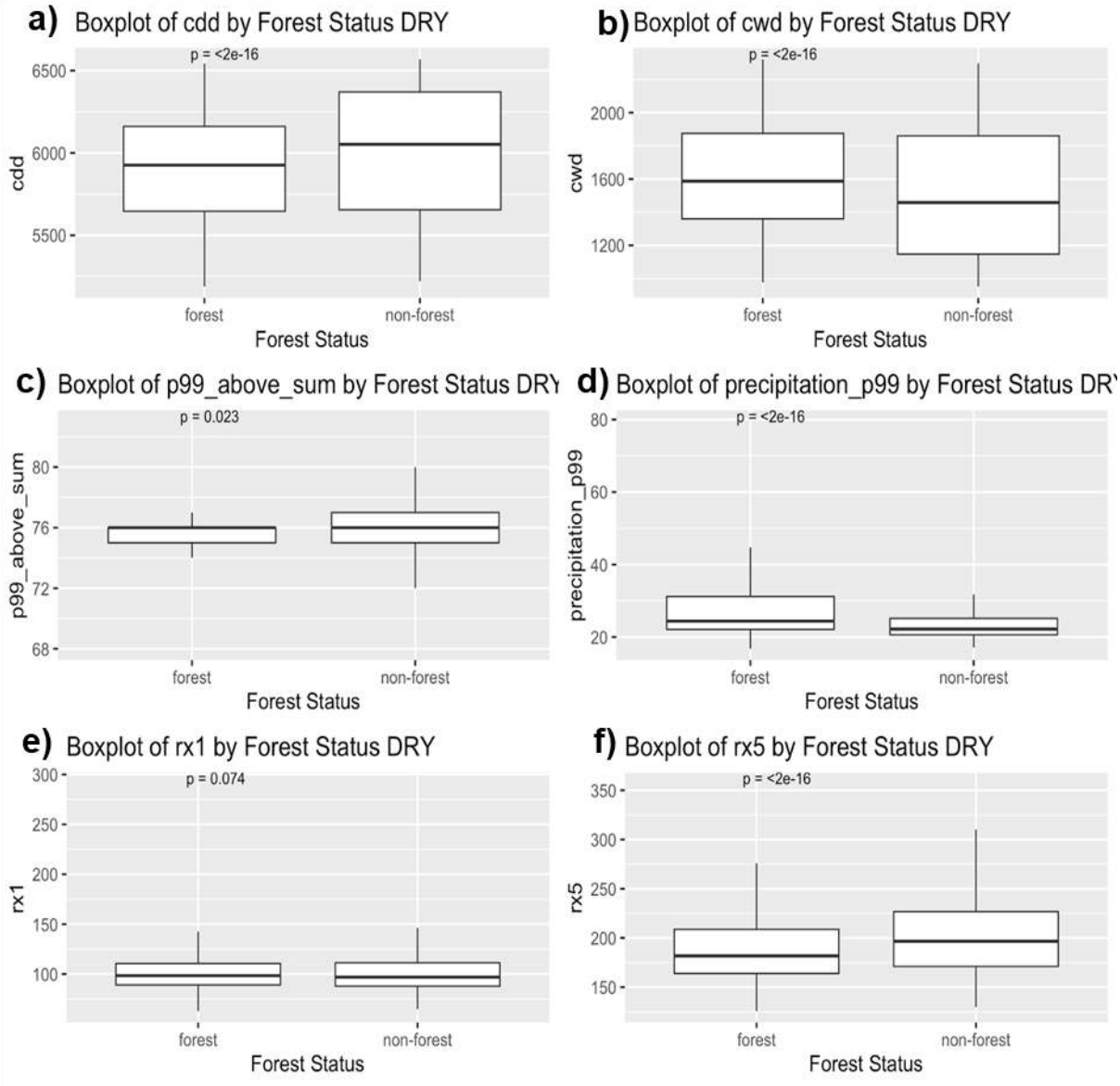
The variable above_p99, representing the frequency of extremely high precipitation events, showed a very weak but statistically significant negative correlation with forest cover ($r = -0.029$, $p = 0.004$). Meanwhile, RX1 (maximum 1-day precipitation) had an even weaker negative correlation ($r = -0.018$) that was not statistically significant ($p = 0.071$), suggesting little to no association between short-duration extreme precipitation and forest cover. Together, these findings highlight that while forest cover is weakly but significantly associated with some hydrometeorological extremes, the relationships are generally modest in magnitude.

These results suggest that forest cover is more strongly associated with the persistence and intensity of wet periods than with individual extreme precipitation events. The significant yet moderate correlations point to the importance of considering the temporal structure of rainfall—such as the frequency of consecutive wet or dry days—when examining the climatic conditions that support or threaten forest cover. These insights may inform land-use planning and ecosystem service modeling in regions where forest dynamics are sensitive to hydrological variability.

3.2. Dry season

Figure 3 below shows the variation in precipitation values (mm or days) in the dry period between the separate rainfall indices in forested areas and deforested areas.

Figure 3 – Boxplot of index values (CDD, CWD, P99, RX1 and RX5) for daily precipitation (dry season) for forest and deforested areas.



Source: Prepared by the authors (2023)

Regarding the CDD indices (Fig. 3a), the results show a slightly lower average number of consecutive dry days in forested areas compared to deforested areas. In relation to the amplitude of consecutive dry days, forest areas and deforested areas show a certain similarity, however with a variation in the average amplitude higher in areas without forest.

For the CWD index (Fig. 3b), the results show a slightly higher average number of consecutive wet days in forested areas compared to deforested areas. In relation to the range of consecutive wet days, there was a slightly higher range of day values for forested areas compared to deforested areas, which showed a smaller range of days.

For the maximum accumulated in one day (RX1), the results show in Fig. 3e a similar average precipitation volume and amplitude (maximum and minimum) in forested areas and deforested areas. For the maximum accumulated over five days (RX5), the results show in Fig. 3f a slightly lower average precipitation volume in forested areas and a slightly higher average volume in deforested areas. The amplitude of the values (maximum and minimum) showed a superior behavior of the maximum values in areas without forest compared to areas with forest that presented smaller amplitudes.

Finally, the results for the indices (P99) of extreme precipitation (volume and days) show in Fig. 3c a similar average of extreme days for both types of land use, but with a greater amplitude in areas without forest. For the average volumes of extreme precipitation (Fig. 3d), forested areas show a slightly higher average value compared to deforested areas, which showed a slightly lower average value. In terms of amplitude of the extreme volume of precipitation, forest areas have a greater maximum amplitude than deforested areas.

In general, forest vegetation has the capacity to influence daily precipitation such as the average reduction of consecutive dry days, the average increase in consecutive wet days, the average reduction in the volume of rain accumulated in five days and, finally, the increase average extreme volume and reduction in the range of days of extreme rain, especially in the dry period. On the other hand, the area without forest vegetation contributes, mainly in the dry period, to the average increase in the number of consecutive days of drought, reduction of consecutive wet days, average increase in the volume and maximum amplitude of rainfall accumulated in five days and for ultimately, an increase in the amplitude of the number of extreme days and a reduction in the extreme volume of precipitation.

4. DISCUSSION

The precipitation regimen in the Xingu watershed is an important aspect of the regional climate and has significant implications for the hydrological cycle and ecosystem dynamics in the area. Several factors influence the precipitation patterns in this watershed, including geographic location, topography, atmospheric circulation patterns, and land cover (Rizzo *et al*., 2020).

The presence of mountain ranges, such as the Serra do Cachimbo, can cause orographic effects, leading to enhanced rainfall on windward slopes and rain shadow areas on the

leeward side. The interaction between the prevailing winds and the topography contributes to the formation of localized convective systems, which can result in intense rainfall events in certain areas (Wang *et al*., 2018).

Atmospheric circulation patterns also have a significant impact on the precipitation regime in the Xingu watershed. The region is influenced by the South Atlantic Convergence Zone (SACZ), a prominent feature of the atmospheric circulation in South America. The SACZ is associated with the convergence of moist air masses from the Amazon basin and the Atlantic Ocean, leading to the formation of convective systems and increased precipitation in the Xingu watershed (Sulca; Rocha, 2021; Towner *et al*., 2021).

Deforestation is driven by a combination of factors in the Xingu watershed, including agricultural expansion, logging, infrastructure development, and land speculation. The expansion of agriculture often involves clearing large areas of forests, leading to changes in land cover and subsequent impacts on the regional climate. Land cover changes, particularly deforestation and land-use practices, can affect the precipitation patterns in the Xingu watershed (Rizzo *et al*., 2020).

Deforestation reduces evapotranspiration and alters surface roughness, leading to changes in the local moisture recycling and atmospheric circulation patterns. Haghtalab *et al*., (2020) found that deforested areas in the Amazon watershed experience reduced rainfall compared to forested areas, indicating the importance of preserving the Amazon rainforest to maintain the regional precipitation regime, especially in the Tocantins region (Haghtalab *et al*., 2020).

Deforestation can result in changes in the properties of the Earth's surface, influencing precipitation patterns in the Xingu basin. One important aspect is the change in albedo, which refers to the amount of solar radiation reflected by the Earth's surface. Deforestation leads to a decrease in albedo, as forests have a higher reflectivity compared to cleared land. This decrease in albedo can result in increased absorption of solar radiation, leading to higher surface temperatures and potentially altering local atmospheric circulation patterns.

Deforestation also affects the ruggedness or surface roughness of the land. Forests typically have a complex structure with a dense canopy, which creates resistance to wind flow. When forests are cleared, the surface becomes smoother, reducing the roughness. This

change in ruggedness can impact the vertical mixing of air masses, affecting cloud formation and precipitation processes.

Another important factor influenced by deforestation is evapotranspiration, which is the combined process of water evaporation from the surface and transpiration by plants. Forests have high evapotranspiration rates due to the abundance of vegetation and moisture availability. When deforestation occurs, evapotranspiration is reduced, leading to changes in the local moisture recycling and moisture availability for cloud formation and precipitation (De Sales *et al*., 2020).

5. CONCLUSIONS

The Xingu watershed has been undergoing the transformation of its forest area due to the advance of deforestation in some regions over the last few decades. These changes can affect the rainfall regime, increasing extreme events over the basin throughout its climatic seasonality.

For the trends of rainfall in the Xingu basin, some changes were observed in the rainfall regime (millimeters and number of days) during the dry season. On the other hand, the trends during the dry period appreciated about 63.6% neutrality and 36.3% reduction in rainfall. All stations that presented statistical significance presented a decreasing trend.

Spatially, trends in rainfall indices (CDD, CWD, RX1, RX5 and p99) changed in some regions of the study area. For the dry period, consecutive dry days increased in the north-south portion and consecutive wet days in the central part of the basin. The maximum accumulated in one and five days shows an increase in the southeast portion and extreme rainfall in the northeast portion.

Given this scenario, the deforested rules within the basin may experience an increase in more extreme events in terms of volume (mm) of rain and a longer drought during the dry season. On the other hand, forest regions can contribute to the reduction of more extreme volumes of rain with an increase in consecutive wetter days.

ACKNOWLEDGEMENTS

The author R.M.M. would like to thank the Pro-Rectory of Graduate Studies and Research of the Federal University of Rondônia for financial support through the Call 004/2024/DPESQ/PROPESQ/UNIR.

REFERENCES

ALVARES, C. A. et al. Köppen's climate classification map for Brazil. **Meteorologische Zeitschrift**, 711–728. 2013. https://doi.org/10.1127/0941-2948/2013/0507

CAVALCANTE, R. B. L. et al. Evaluation of extreme rainfall indices from CHIRPS precipitation estimates over the Brazilian Amazonia. **Atmospheric Research**, v. 238, p. 104879, 2020.

DE MORAES CORDEIRO, A. L.; BLANCO, C. J. C. Assessment of satellite products for filling rainfall data gaps in the Amazon region. **Natural Resource Modeling**, [s. l.], v. 34, n. 2, p. e12298, 2021.

DE SALES, F. et al. Impacts of Protected Area Deforestation on Dry-Season Regional Climate in the Brazilian Amazon. **Journal of Geophysical Research: Atmospheres**, [s. l.], v. 125, n. 16, p. e2020JD033048, 2020.

DIAS, L. C. P. et al. Effects of land cover change on evapotranspiration and streamflow of small catchments in the Upper Xingu River Basin, Central Brazil. **Journal of Hydrology: Regional Studies**, [s. l.], v. 4, p. 108–122, 2015.

FUNK, C. et al. The climate hazards infrared precipitation with stations—a new environmental record for monitoring extremes**. Scientific Data**, [s. l.], v. 2, n. 1, p. 150066, 2015.

HAGHTALAB, N. et al. Evaluating spatial patterns in precipitation trends across the Amazon basin driven by land cover and global scale forcings. **Theoretical and Applied Climatology**, [s. l.], v. 140, n. 1, p. 411–427, 2020.

LUCAS, E. W. M. et al. Trends in climate extreme indices assessed in the Xingu river basin - Brazilian Amazon. **Weather and Climate Extremes**, [s. l.], v. 31, p. 100306, 2021.

MAPBIOMAS BRASIL. **Coleção 7.1 da Série Anual de Mapas de Cobertura e Uso de Solo do Brasil**. Disponível online: https://mapbiomas.org/colecoes-mapbiomas-1?cama_set_language=pt-BR. Acessado em 19/03/2023.

MU, Y.; BIGGS, T.; SHEN, S. S. P. Satellite-based precipitation estimates using a dense rain gauge network over the Southwestern Brazilian Amazon: Implication for identifying trends in dry season rainfall. **Atmospheric Research**, [s. l.], v. 261, p. 105741, 2021.

PACA, V. H. M. et al. Variability of trends in precipitation across the Amazon River basin determined from the CHIRPS precipitation product and from station records. **Water**, v. 12, n. 5, p. 1244, 2020.

RIZZO, R. et al. Land use changes in Southeastern Amazon and trends in rainfall and water yield of the Xingu River during 1976–2015. **Climatic Change**, [s. l.], v. 162, n. 3, p. 1419–1436, 2020.

SOARES-FILHO, B. et al. Forest fragmentation, climate change and understory fire regimes on the Amazonian landscapes of the Xingu headwaters. **Landscape Ecology**, [s. l.], v. 27, n. 4, p. 585–598, 2012.

DE SOUZA, M. B. et al. Dinâmica de uso e cobertura da terra no município de São Félix do Xingu, Estado do Pará, Brasil. **Research, Society and Development**, v. 9, n. 10, p. e4889108791-e4889108791, 2020.

SULCA, J. C.; ROCHA, R. P. da. Influence of the Coupling South Atlantic Convergence Zone-El Niño-Southern Oscillation (SACZ-ENSO) on the Projected Precipitation Changes over the Central Andes. **Climate**, [s. l.], v. 9, n. 5, p. 77, 2021.

TATE, Robert F. Correlation between a discrete and a continuous variable. Point-biserial correlation. **The Annals of mathematical statistics**, v. 25, n. 3, p. 603-607, 1954.

TOWNER, J. et al. Influence of ENSO and tropical Atlantic climate variability on flood characteristics in the Amazon basin. **Hydrology and Earth System Sciences**, [s. l.], v. 25, n. 7, p. 3875–3895, 2021.

WANG, C. et al. Integrated Effects of Land Use and Topography on Streamflow Response to Precipitation in an Agriculture-Forest Dominated Northern Watershed. **Water**, [s. l.], v. 10, n. 5, p. 633, 2018.